JACS
JOURNAL OF THE AMERICAN CHEMICAL SOCIETY
Article
pubs.acs.org/JACS

Mechanistic Rationalization of Unusual Kinetics in Pd-Catalyzed C−H Olefination

Ryan D. Baxter, David Sale, Keary M. Engle, Jin-Quan Yu, and Donna G. Blackmond*

Department of Chemistry, The Scripps Research Institute, La Jolla, California 92037, United States

Supporting Information

ABSTRACT: Detailed kinetic studies and novel graphical manipulations of reaction progress data in Pd(II)-catalyzed olefinations in the presence of mono-*N*-protected amino acid ligands reveal anomalous concentration dependences (zero order in *o*-CF_3-phenylacetic acid concentration, zero order in oxygen pressure, and negative orders in both olefin and product concentrations), leaving the catalyst concentration as the sole positive driving force in the reaction. NMR spectroscopic studies support the proposal that rate inhibition by the olefinic substrate and product is caused by formation of reversible off-cycle reservoirs that remove catalyst from the active cycle. NMR studies comparing the interaction between the catalyst and substrate in the presence and absence of the ligand suggest that weak coordination of the ligand to Pd prevents formation of an inactive mixed acetate species. A fuller understanding of these features may lead to the design of more efficient Pd(II) catalysts for this potentially powerful C−H functionalization reaction.

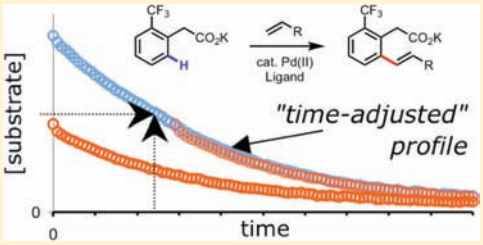

INTRODUCTION

The study of Pd-catalyzed C−H activation for a diverse range of carbon−carbon and carbon−heteroatom bond-forming reactions has become a vibrant area of research.[1] The development of catalyst−ligand systems that can improve reactivity[2−4] and positional selectivity[2a,5] for a broad range of synthetically useful substrates has been hampered by lack of mechanistic understanding. Complications in C−H functionalization reactions arise from the fact that Pd(II) in the absence of a ligand often exists as a mixture of monomeric and higher order species, all potentially participating in the catalytic cycle. A recently uncovered Pd(II)/ligand system for C−H olefination (Scheme 1) offers a catalytic platform for our focus on the reaction kinetics to provide mechanistic clues to aid in the design of improved catalysts and reaction protocols.

Scheme 1. C−H Activation of Arylacetic Acids

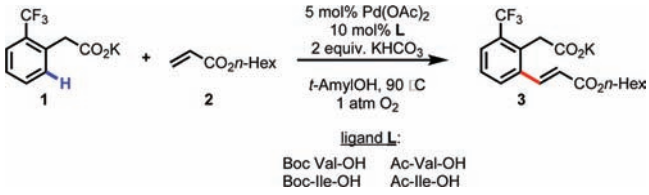

The Pd(II)-catalyzed C−H olefination of substrates such as *o*-(trifluoromethyl)phenylacetic acid **1** has been proposed to follow the basic catalytic shown in Scheme 2.[2c] Following coordination of the substrate **1** to Pd(II), carboxylate-directed *ortho*-C−H cleavage takes place to form a cyclopalladated intermediate. Olefin coordination followed by 1,2-migratory insertion forms the new C−C bond, and *β*-hydride elimination releases the product. Reductive elimination followed by reoxidation closes the catalytic cycle with regeneration of Pd(II). A hydrogen atom abstraction mechanism for reoxidation with O_2 is also possible.

Scheme 2. *ortho*-C−H Olefination of Phenylacetic Acids

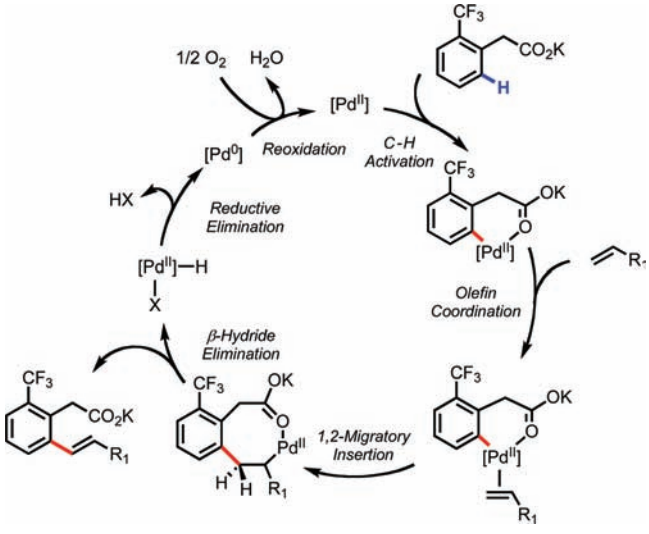

While previous work demonstrated that addition of mono-*N*-protected amino acid ligands provided higher yields in significantly shorter reaction times, the precise role of the ligand was not made clear. A recent computational study examining enantioselective C−H activation using these catalysts pointed to a pathway initiated by N−H cleavage followed by *ortho*-C−H activation rather than a direct C−H

Received: August 12, 2011
Published: February 10, 2012

   dx.doi.org/10.1021/ja207634t | *J. Am. Chem. Soc.* 2012, 134, 4600−4606

activation route.[6] However, none of this work provides evidence to support the simplified mechanism presented in Scheme 2 and the role of the ligand in these elementary steps. We report here detailed kinetic studies on the *ortho*-C−H olefination of phenylacetic acids using $Pd(OAc)_2$ in the presence of mono-*N*-protected amino acid ligands (Scheme 1), which have previously been demonstrated to accelerate the reaction rate.[2,6] In- situ reaction monitoring using ReactIR spectroscopy and NMR spectroscopy presents concentration dependences, identifies the resting state of the catalyst, and presents a modified mechanistic proposal to clarify several features of the putative mechanism for these reactions.

RESULTS AND DISCUSSION

Kinetic Studies. Our kinetic protocol features experiments probing catalyst stability and the concentration dependences of the substrates that allow interrogation of the mechanism shown in Scheme 2 in the presence of the ligand and provide clarification of several mechanistic features not highlighted previously. ReactIR spectroscopy was employed for continuous monitoring of reaction progress.[7] Figure 1 compares the kinetic

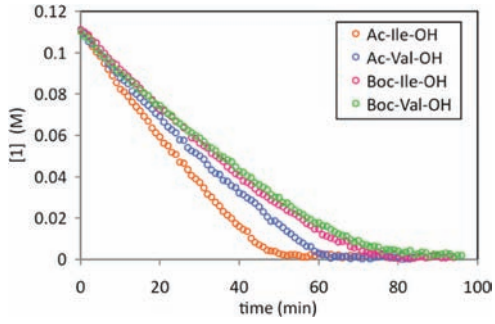

Figure 1. Concentration of substrate **1** as a function of time for the reaction of Scheme 1 carried out using four different ligand/protecting group combinations. $[\mathbf{1}]_0$ = 0.11 M; $[\mathbf{2}]_0$ = 0.44 M; [Pd] = 5.6 mM; Pd:L = 1:2.

profiles for reactions carried out under identical conditions using four ligand/protecting group systems. The relative reactivities of the ligand/protecting group systems are given in eq 1. The most reactive case differed from the least reactive by a factor of ca. 1.5, and the basic form of the kinetic profile is similar in all cases. These rates are considerably faster (by more than 10-fold) than the reaction in the absence of ligand, as reported previously.[2c] Since similar results were obtained for all four ligand systems, representative results are shown here for the Boc-Val-OH system; data for the others are found in the Supporting Information.

$$\text{reaction rate: Ac-Ile-OH} > \text{Ac-Val-OH} > \text{Boc-Val-OH} \approx \text{Boc-Ile-OH} \quad (1)$$

For all four ligand systems, the reaction was found to be first order in [Pd], as shown in Figure 2. Since the data in Figure 1 reveal overall kinetics of nearly zero order, the rates in Figure 2 may be obtained from the slopes of the concentration profiles of reactions carried out under identical conditions except for varying the catalyst concentration.

Identical rates were observed using Pd:ligand concentrations of 1:1 and 1:2,[7] supporting the proposal that a single ligand coordinates Pd in the catalytic cycle. Experiments varying the

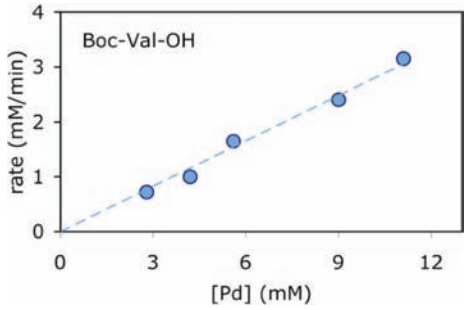

Figure 2. Reaction rate measured from the slope of ReactIR concentration versus time profiles for the reaction of Scheme 1. Reactions carried out at different Pd (Pd:ligand = 1:2) with $[\mathbf{1}]_0$ = 0.080 M; $[\mathbf{2}]_0$ = 0.302 M. All other conditions as in Scheme 1.

stirring speed (200−600 rpm) and oxygen pressure (15−100 psi) reveal that the reaction rate is zero order in oxygen concentration.[7] The reaction was observed to proceed at similar rates in NMR tubes using indigenous oxygen present in nondegassed solvent. These observations confirm that Pd reoxidation is not the slow step in the cycle, suggesting that a prior step in the cycle controls the rate.

The concentration dependences and the stability of the catalyst system may be probed using the "different excess" and "same excess" protocols, respectively, of Reaction Progress Kinetic Analysis (RPKA).[7,8] A brief description of these protocols follows. In a reaction as in Scheme 1 exhibiting 1:1 stoichiometry between two substrates, the "excess" [**e**] is defined as the *difference* in concentrations of two reactants, in this case **1**, the arylacetic acid salt, and **2**, the olefin (eq 2). The parameter excess has units of concentration and is invariable over the course of a catalytic reaction, and hence [**e**] is fixed by the initial concentrations chosen for a reaction.

$$\text{excess} = [\mathbf{e}] = [\mathbf{2}]_0 - [\mathbf{1}]_0 = [\mathbf{2}] - [\mathbf{1}] \quad (2)$$

The logic of how kinetic information is extracted from these protocols may be illustrated by considering a simple model reaction rate expression. The rate of most reactions is dependent on the concentrations of the reactants in some form. In initial studies of any new reaction or in any case where the mechanism is uncertain, an empirical description of the concentration driving forces may be written in what is known as the power-law form, where x equals the order in **1** and y equals the order in **2** (eq 3). The experimentally determined magnitudes of x and y may then be used to provide clues about the detailed reaction mechanism.

$$\text{rate} = k\cdot[\mathbf{1}]^x\cdot[\mathbf{2}]^y \quad (3)$$

When fit to data from catalytic or other multistep reactions, non-integer values of reaction orders in substrate concentrations are often obtained, which are not directly related to the molecularity of any individual elementary step in the mechanism. Power-law expressions may be employed as a simplification of the more complex algebraic form of Michaelis−Menten catalytic kinetic rate expressions. The relationship between the two forms, including use of the empirical form to delineate the fundamental mechanism, were recently demonstrated for a proline-mediated aldol reaction.[9]

Since phenylacetic acid **1** and olefin **2** concentrations are related to each other through the definition of excess, the rate expression of eq 3 may be written in terms of a single concentration variable, as shown in eqs 4 and 5. Equation 5 thus reveals that reaction rate

dx.doi.org/10.1021/ja207634t | J. Am. Chem. Soc. 2012, 134, 4600−4606

may be measured over the course of the reaction by following the concentration of only one of the two substrates.

$$[\mathbf{2}] = [\mathbf{e}] + [\mathbf{1}] \quad (4)$$

$$\text{rate} = k\cdot[\mathbf{1}]^{x}\cdot([\mathbf{e}] + [\mathbf{1}])^{y} \quad (5)$$

It may be shown that data from two experiments carried out at two different values of [**e**] are mathematically sufficient for a unique determination of the reaction orders in two substrates (x and y), which is the theoretical basis of the "different excess" protocol.[8]

Equation 5 also makes it clear that for all reactions carried out at a specific value of [**e**], the same rate should be obtained at the same concentration of **1** regardless of its initial concentration. Thus if two reactions employing the same [**e**] and different initial concentrations of **1** do *not* exhibit the same rate at a given value of [**1**], this result provides a clear indication that a process other than the intrinsic kinetics influences the reaction rate. The most likely candidates include catalyst activation or deactivation and substrate or product inhibition, none of which is accounted for in the intrinsic kinetic rate law. This provides the theoretical basis of the "same excess" protocol for probing catalyst stability and process robustness.[8]

Commonly used kinetic methods typically measure concentrations as a function of time, and raw temporal data must be manipulated mathematically in order to allow a comparison of reaction rate as a function of substrate concentration, as dictated by RPKA analysis in both the "same excess" and "different excess" protocols. Differentiation of temporal concentration data to obtain rate often results in increased noise in the data, a drawback that potentially hampers the use of reaction progress data to their fullest extent in many mechanistic studies. However, as presented below, simple graphical manipulations of the temporal profiles may be used in some cases to provide kinetic information about catalyst stability and concentration dependences without the requirement of mathematical manipulations.

We first illustrate this treatment for the "same excess" protocol for the reaction of Scheme 1. Figure 3 shows

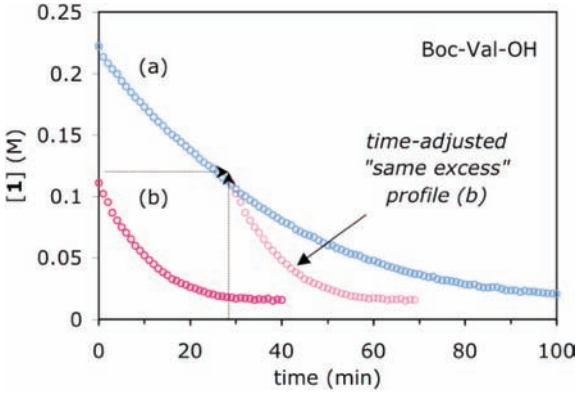

Figure 3. Concentration of substrate **1** as a function of time for the reaction of Scheme 1 carried out using the "same excess" protocol: runs (a) and (b) have different initial concentration of substrates **1** and **2**, with the *difference* between the two (defined as the excess = $[\mathbf{2}]_0 - [\mathbf{1}]_0$) held the same. The time-adjusted profile for run (b) has the same [**1**] and [**2**] as run (a) has at the point marked by the arrows. All other conditions as given in Scheme 1.

concentration profiles for two "same excess" experiments. The temporal concentrations of **1** and **2** in run (a) are identical to those in run (b) at the time point marked by the arrows in the figure. Comparison of the profiles of these two reactions from a point of identical concentrations of the two substrates is made possible by shifting curve (a) over to the time point marked. Two reactions under identical conditions should give identical temporal profiles from this time point onward. However, it is easily seen that the reaction of curve (b) proceeds faster than that of (a) from this point, even though the two exhibit identical concentrations at this point. The fact that the "time-adjusted" profile from reaction (a) does not overlay onto that of reaction (b) from the marked time point onward confirms that some process other than the intrinsic kinetics related to the temporal substrate concentrations [**1**] and [**2**] contributes to the observed reaction rate.

We consider that there are two key differences between these reactions at the point marked by the arrows shown in Figure 3, despite the fact that substrate concentrations [**1**] and [**2**] are identical at this point: (1) the reaction in run (a) has undergone a number of turnovers prior to reaching concentrations that are identical to the initial concentrations of the reaction in run (b), which has not yet completed any turnovers at the point marked by the arrows; and (2) the reaction mixture for run (a) contains product from these previous turnovers, whereas the reaction mixture in newly initiated run (b) contains only substrates and catalyst at the time marked by the arrows. Therefore the most likely possibilities to rationalize the lack of overlay between the two curves from the time-adjusted point onward in Figure 3 are either that catalyst deactivation has occurred in run (a) or that the catalyst is sensitive to product inhibition.

This latter proposition may be tested by carrying out a reaction under the conditions of run (b) with the appropriate quantity of product added so that the concentrations of not only substrates **1** and **2** but also that of *product* **3** are matched to those for run (a) at the time-adjusted point. Figure 4

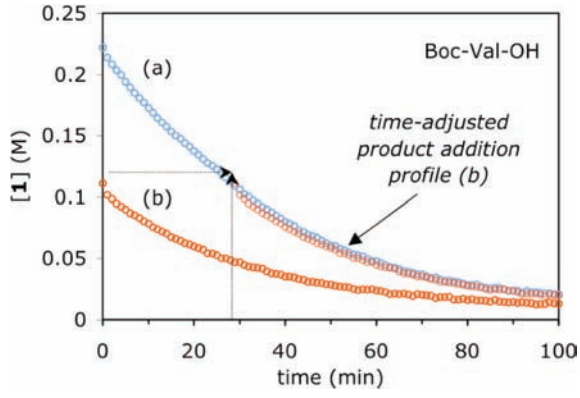

Figure 4. Concentration of substrate **1** as a function of time for the reaction of Scheme 1 carried out using the "same excess" protocol as in Figure 5, with product addition: run (b) has added product to match the product concentration of run (a) at the point of the time adjustment (shown by arrows). All other conditions as given in Scheme 1.

compares the concentration profile for a reaction using this product addition protocol with that of run (a) from Figure 3. The results reveal excellent superposition of the time-adjusted same excess experiment with the product added same excess experiment. Overlay between the two curves shown in Figure 4 demonstrates that the two reactions exhibit the same rate, providing clear evidence that the catalyst system is sensitive to

dx.doi.org/10.1021/ja207634t | J. Am. Chem. Soc. 2012, 134, 4600–4606

product inhibition. In addition, this figure confirms the robustness of the system to other irreversible catalyst deactivation processes, which are clearly negligible under these conditions.

The use of temporal concentration profiles using the "different excess" protocol[8] in reaction progress kinetics is illustrated in Figures 5−7. Again, while the standard RPKA analysis involves consideration of the data in the form of reaction rate as a function of concentration, we demonstrate

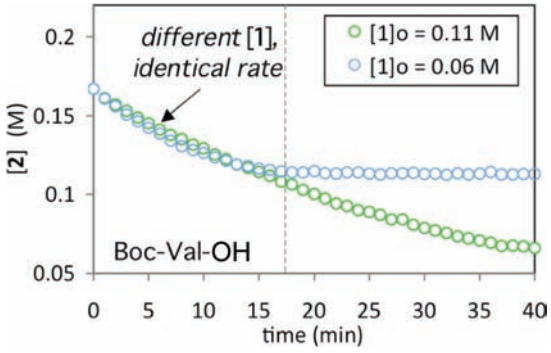

Figure 5. Concentration of substrate **2** as a function of time for the reaction of Scheme 1 carried out using $[\mathbf{2}]_0$ = 0.167 M and two different initial concentrations of substrate **1**: $[\mathbf{1}]_0$ = 0.11 M; $[\mathbf{1}]_0$ = 0.06 M. The dashed line shows where the reaction in blue circles ends due to full consumption of **1** while the reaction in green circles continues due to its higher initial concentration of **1**. All other conditions as given in Scheme 1.

that for particular simplified cases, significant kinetic information may be extracted directly from the temporal concentration profiles without prior conversion to rate. Figure 5 shows the kinetic profile for runs carried out with identical $[\mathbf{2}]_0$ and different initial concentrations of **1**. The time course of $[\mathbf{2}]$ during the two reactions is identical up to the point of complete consumption of **1** for the reaction with lower $[\mathbf{1}]_0$. The fact that these profiles overlay at different values of $[\mathbf{1}]$ indicates that the reaction rate is independent of $[\mathbf{1}]$.

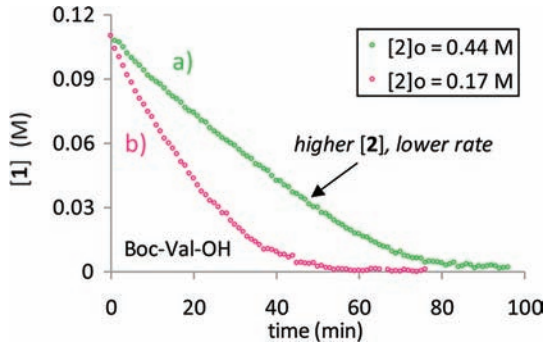

Figure 6. Concentration of substrate **1** as a function of time for the reaction of Scheme 1 carried out using two different initial concentrations of substrate **2**, showing a slower rate for higher $[\mathbf{2}]$. All other conditions as given in Scheme 1.

Figure 6 shows two experiments carried out using the opposite protocol, that is, with identical $[\mathbf{1}]_0$ and different initial concentrations of **2**. Higher $[\mathbf{2}]_0$ results in a slower reaction, indicating an unusual *negative* dependence on the olefinic substrate $[\mathbf{2}]$. In this case the magnitude of the exponent y may be

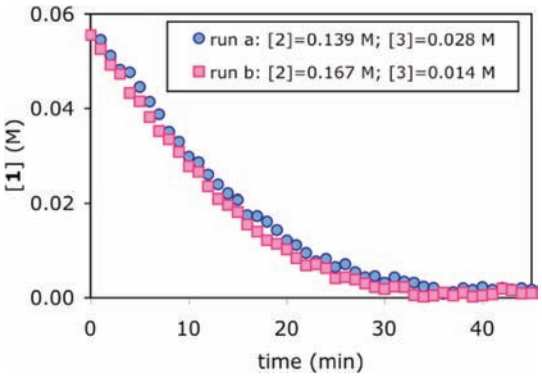

Figure 7. Concentration profiles for reactions probing the relative rate suppression caused substrate **2** and product **3**.[7]

determined qualitatively for these conditions by comparing initial slopes of the temporal profiles (eq 6), giving $y \approx -0.5$.

$$\log\left[\frac{(\text{rate})_a}{(\text{rate})_b}\right] = \log\left[\frac{(\text{slope})_a}{(\text{slope})_b}\right] = y \log\left[\frac{[\mathbf{2}]_a}{[\mathbf{2}]_b}\right] \quad (6)$$

Several further kinetic experiments allow estimation of an empirical order describing product inhibition. Figure 7 shows time course profiles for two runs that exhibit nearly identical rates, carried out with different concentrations of substrate **2** and added product **3**. The observed rates for run (a) and run (b) are equal (eq 7). This allows an empirical power-law rate expression incorporating product inhibition to be written as shown in eq 8. Inserting concentrations from the data in Figure 7 and the previously obtained value $y = -0.5$, we obtain a value of $z = -0.13$.

$$(\text{rate})_a = (\text{rate})_b \quad (7)$$

$$(k'[\mathbf{2}]^y \cdot [\mathbf{3}]^z)_a = (k'[\mathbf{2}]^y \cdot [\mathbf{3}]^z)_b \quad (8)$$

Taken together, these kinetic results present an intriguing mechanistic puzzle. Most catalytic cycles exhibit positive order kinetics in one or more substrate concentrations as well as in catalyst concentration, and these quantities are generally considered to act as driving forces for the reaction. In this coupling reaction, however, *neither* of the substrates **1** or **2** nor the $[O_2]$ required to regenerate the catalyst exhibits positive order kinetics, and in fact, both one of the substrates as well as the reaction product itself are found to *suppress* the reaction rate. Thus the catalyst provides the only positive concentration driving force in this reaction. The generally accepted mechanism shown in Scheme 2 cannot account for these observations.

Next we may transform the empirical power-law form into a more rigorous proposed steady-state catalytic rate expression by proposing a mathematical description of elementary steps in a modified reaction network that takes into account all of these kinetic observations. The basic elementary steps corresponding to one proposed network, along with mathematical descriptions of the intermediate species' concentrations under steady-state conditions, are given in Scheme 3. While the kinetic data cannot provide proposals concerning the nature of these intermediate species, this mathematical treatment may then be used to inform further spectroscopic experiments probing the identity of the proposed species.

Zero order kinetics in substrate **1** suggests a pre-equilibrium to form a kinetically meaningful species $\mathbf{I_1}$ with coordination of

dx.doi.org/10.1021/ja207634t | J. Am. Chem. Soc. 2012, 134, 4600−4606

Scheme 3. Elementary Steps and On- and Off-Cycle Intermediates in a Modified Reaction Network[a]

on-cycle:

$$Pd + \mathbf{1} \underset{k_{-1}}{\overset{k_1}{\rightleftarrows}} I_1 \qquad [I_1] = K_{eq,1}[\mathbf{1}][Pd] \qquad K_{eq,1} = \frac{k_1}{k_{-1}}$$

$$I_1 \xrightarrow{k_2} I_2$$

$$I_2 + \mathbf{2} \xrightarrow{k_3} I_3 \qquad [I_2] = \frac{k_2[I_1]}{k_3[\mathbf{2}]} = \frac{k_2}{k_3[\mathbf{2}]} K_{eq,1}[\mathbf{1}][Pd]$$

$$I_3 \xrightarrow{k_4} I_4 + \mathbf{3} \qquad [I_3] = \frac{k_3[I_2][\mathbf{2}]}{k_4} = \frac{k_2}{k_4} K_{eq,1}[\mathbf{1}][Pd]$$

$$I_4 + O_2 \xrightarrow{k_5} Pd \qquad [I_4] = \frac{k_4[I_3]}{k_5[O_2]} = \frac{k_2}{k_5} K_{eq,1} \frac{[\mathbf{1}][Pd]}{[O_2]}$$

off-cycle:

$$I_1 + \mathbf{2} \underset{}{\overset{K_{eq,2b}}{\rightleftarrows}} \mathbf{2b} \qquad [\mathbf{2b}] = K_{eq,2b} K_{eq,1}[\mathbf{1}][\mathbf{2}][Pd]$$

$$I_1 + \mathbf{3} \underset{}{\overset{K_{eq,3b}}{\rightleftarrows}} \mathbf{3b} \qquad [\mathbf{3b}] = K_{eq,3b} K_{eq,1}[\mathbf{1}][\mathbf{3}][Pd]$$

[a]See Supporting Information for derivations.

1 to Pd. The kinetic data indicate that such a species exists non-fleetingly prior to C−H cleavage in a step that forms another intermediate $\mathbf{I_2}$ prior to olefin coordination to form $\mathbf{I_3}$, which eliminates the reaction product **3** and forms the reduced Pd species $\mathbf{I_4}$. The observation of zero order kinetics in $[O_2]$ indicates that the only steps prior to reoxidation of I_4 are potentially kinetically meaningful. Negative dependences on olefin substrate [**2**] and product olefin [**3**] suggest off-cycle binding interactions between these species and the catalyst forming **2b** and **3b** that effectively decrease the active Pd content within the cycle. $K_{eq,2b}$ and $K_{eq,3b}$ represent binding constants between $\mathbf{I_1}$ and **2** or **3**, respectively. It is important to note that the off-cycle reservoir species **2b** and **3b** must also contain **1** in order to reconcile the zero order dependence on [**1**], as demonstrated in the equations below.

The rate of reaction may be written as the first irreversible step in the network, which is suggested to be the C−H activation step to form $\mathbf{I_2}$ (eq 9). Intermediates formed on the cycle after this step will be present in low concentrations relative to the other catalytic species (i.e., $[\mathbf{I_3}]$, $[\mathbf{I_4}] \ll [\mathrm{Pd}]$, $[\mathbf{I_1}]$) and may be neglected in the catalyst mass balance (eq 10).

$$\text{rate} = k_2[\mathbf{I_1}] = k_2 K_{\mathrm{eq},\mathbf{1}}[\mathbf{1}][\mathrm{Pd}] \tag{9}$$

$$\begin{aligned}[\mathrm{Pd}]_{\mathrm{total}} &\approx [\mathrm{Pd}] + \mathbf{I_1} + \mathbf{2b} + \mathbf{3b} \\ &= [\mathrm{Pd}](1 + K_{\mathrm{eq},\mathbf{1}}[\mathbf{1}](1 + K_{\mathrm{eq},\mathbf{2b}}[\mathbf{2}] \\ &\quad + K_{\mathrm{eq},\mathbf{3b}}[\mathbf{3}]))\end{aligned} \tag{10}$$

Solving for [Pd] in the mass balance and substituting into the rate law of eq 9 gives the simplified rate law of eq 11.

$$\text{rate} = \frac{k_2 K_{\mathrm{eq},\mathbf{1}}[\mathbf{1}][\mathrm{Pd}]_{\mathrm{total}}}{(1 + K_{\mathrm{eq},\mathbf{1}}[\mathbf{1}](1 + K_{\mathrm{eq},\mathbf{2b}}[\mathbf{2}] + K_{\mathrm{eq},\mathbf{3b}}[\mathbf{3}]))} \tag{11}$$

Making an assumption that the concentration of $\mathbf{I_1}$ is much greater than that of the free Pd within the cycle (i.e., $[\mathbf{I_1}] \gg [\mathrm{Pd}]$) simplifies the expression to that of eq 12. The validity of this assumption is supported by the fact that this form of the steady-state rate law reconciles the kinetic dependences observed, that is, zero order kinetics in [**1**] together with negative order kinetics in [**2**] and [**3**].

$$\text{rate} = \frac{k_2[\mathrm{Pd}]_{\mathrm{total}}}{(1 + K_{\mathrm{eq},\mathbf{2b}}[\mathbf{2}] + K_{\mathrm{eq},\mathbf{3b}}[\mathbf{3}])} \tag{12}$$

The data in Figure 7 from reactions carried out with different concentrations of **2** and **3** also allow estimation of the relative stability of the two reservoir species **2b** and **3b**. Since the two reactions exhibited equal rates, we may equate the catalytic rate law of eq 12 written for conditions of experiment (a) equal to that written for conditions of experiment (b) in Figure 7. Canceling common terms provides eq 13, which may be rearranged as eq 14. This treatment reveals that binding of the catalyst to product to form **3b** is ca. two times stronger than binding of the catalyst to olefin to form **2b**.

$$\begin{aligned}&(K_{\mathrm{eq},\mathbf{3b}}\cdot[\mathbf{3}] + K_{\mathrm{eq},\mathbf{2b}}\cdot[\mathbf{2}])_{\mathrm{a}} \\ &\quad = (K_{\mathrm{eq},\mathbf{3b}}\cdot[\mathbf{3}] + K_{\mathrm{eq},\mathbf{2b}}\cdot[\mathbf{2}])_{\mathrm{b}}\end{aligned} \tag{13}$$

$$\frac{K_{\mathrm{eq},\mathbf{3b}}}{K_{\mathrm{eq},\mathbf{2b}}} = \frac{[\mathbf{2}]_{\mathrm{b}} - [\mathbf{2}]_{\mathrm{a}}}{[\mathbf{3}]_{\mathrm{a}} - [\mathbf{3}]_{\mathrm{b}}} \approx 2 \tag{14}$$

We are now in a position to compare the empirical power-law form first developed as eq 8 with the steady-state catalytic form of eq 12 developed from the mechanistic treatment of Scheme 3, as shown in eq 15. The usefulness of the empirical power-law form of the rate law is 2-fold: first, the empirical assessment of the magnitude of various concentration driving forces aids in proposing the elementary steps to account for the observed behavior and hence may be used as a mechanistic tool; and second, the power-law form provides facility in selecting conditions for practical scale-up and application of this chemistry.

$$\begin{aligned}\text{rate} &= \frac{k_2[\mathrm{Pd}]_{\mathrm{total}}}{(1 + K_{\mathrm{eq},\mathbf{2b}}[\mathbf{2}] + K_{\mathrm{eq},\mathbf{3b}}[\mathbf{3}])} \\ &\approx k'\cdot[\mathbf{2}]^{-0.5}\cdot[\mathbf{3}]^{-0.13}\cdot[\mathrm{Pd}]_{\mathrm{total}}\end{aligned} \tag{15}$$

The first order dependence on Pd(II) concentration shown in either form of the rate law is consistent with involvement of a well-defined mononuclear Pd(II)−amino acid complex as the active catalyst. The presence of off-cycle catalyst reservoirs implies that the active steady-state concentration of Pd within the catalytic cycle remains low throughout the reaction. A consequence of sequestering Pd in off-cycle reservoirs is that the lower on-cycle exposure of Pd enables C−H activation and subsequent steps without promoting irreversible deactivation of Pd, for example, to form reduced Pd^0 in the form of Pd black. Thus off-cycle reservoirs that suppress rate may play a positive

dx.doi.org/10.1021/ja207634t | J. Am. Chem. Soc. 2012, 134, 4600−4606

role in maintaining an effective steady-state concentration of active catalyst species.[11] Further development of this type of ligand scaffold for well-defined monomeric Pd catalysts, including tailoring more reactive ligands through tuning the steric and electronic properties, may help to optimize reactivity while maintaining the beneficial aspects of competitive olefin binding prior to the C−H cleavage step.

Spectroscopic Studies. The kinetic studies reveal the mathematical form of the reaction rate, suggest a plausible set of elementary steps, and provide clues to the nature of on- and off-cycle intermediates. We turn to NMR spectroscopic probing of this system first to probe the role of the ligand in rate acceleration and then to propose structures for intermediate species that are consistent with these kinetics and other experimental and computational results.

NMR spectra of the interaction of $Pd(OAc)_2$ and substrate **1** in the absence of ligand revealed the formation of a new species. Figure 8 shows EXSY correlation indicating equilibrium

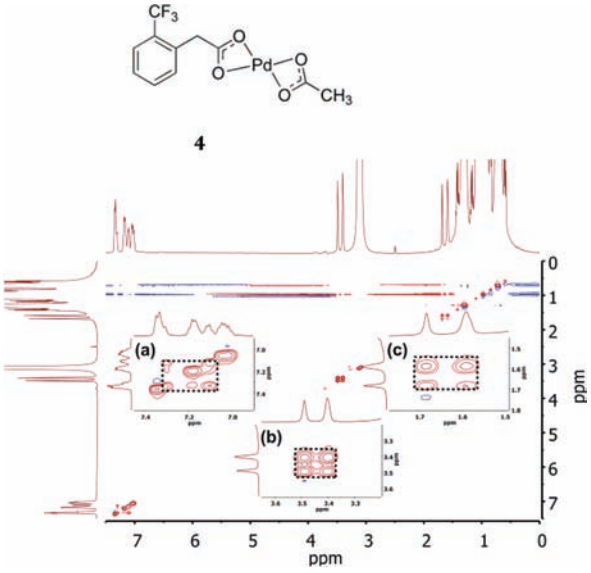

Figure 8. 500 MHz NOESY 2-D spectrum of **1** (0.1 M), $Pd(OAc)_2$ (0.03 M), and $KHCO_3$ (0.1 M) in *t*-AmylOH at 70 °C. Insets highlighting chemical exchange between protons in different regions: (a) 6.9−7.4 ppm, aromatic protons, (b) 3.4−3.7 ppm, benzylic protons, (c) 1.5−1.8 ppm, acetyl protons.

between the free substrate and the new species. These spectra suggest a 1:1 ratio between two different acetate species. This suggests that displacement of one acetate from the Pd precursor by the carboxylate of **1** results in a new mixed-acetate species **4**. This new species appears to be unaffected by addition of olefin **2**, and very little product is formed after three hours in the absence of the amino acid ligand.

The new species **4** is not formed when the ligand is present in the system. Figure 9 shows ^{1}H NMR spectra of substrates **1** and **2** alone (Figure 9c and a, respectively) and in the presence of $Pd(OAc)_2$ and the mono-*N*-protected ligand Ac-Ile-OH (Figure 9d and b, respectively). Broadening and shifting of peaks result upon addition of **1** to the Pd−ligand system, and a new broad peak appears below 7 ppm (Figure 9d). While no interaction between the olefin **2** and the Pd−ligand system is evident in the absence of substrate **1**, addition of olefin to the Pd−ligand−**1** system causes significant broadening of the olefin peaks (compare Figure 9b and Figure 9e). Reaction turnover

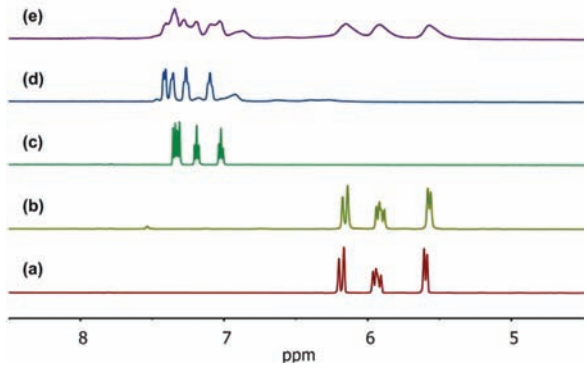

Figure 9. 500 MHz ^{1}H NMR spectra at 70 °C in *t*-AmylOH of (a) **2** (0.1 M), (b) **2** (0.1 M), and $Pd(OAc)_2$ (0.03 M), Ac-Ile-OH (0.03 M), and $KHCO_3$ (0.1 M), (c) **1** (0.1 M), (d) **1** (0.1 M), $Pd(OAc)_2$ (0.03 M), Ac-Ile-OH (0.03 M), and $KHCO_3$ (0.1 M), and (e) **1** (0.1 M), $Pd(OAc)_2$ (0.03 M), Ac-Ile-OH (0.03 M), $KHCO_3$ (0.1 M), and **2** (0.1 M) immediately after the addition of **2**.

begins immediately upon addition of olefin to this system. No evidence of a Pd hydride species was found under any conditions.

These results taken together with those of recent computational studies[6] help to rationalize the role of the ligand in promoting the C−H activation reaction. A mixed acetate Pd complex formed with substrate **1** in the absence of ligand is inactive as a catalyst. Presence of the mono-*N*-protected amino acid ligand prevents formation of this stable complex via weak coordination of the ligand. Computational results suggest that reaction in the presence of ligand may proceed through an N−H activation pathway rather than through direct C−H activation.[6] In the context of our kinetic scenario of Scheme 3, intermediate species $\mathbf{I_1}$ becomes two kinetically indistinguishable species $\mathbf{I_{1a}}$ and $\mathbf{I_{1b}}$ resulting from coordination of **1** to the catalyst followed by N−H activation, as shown in Scheme 4. Prior to N−H activation, the weakly coordinated species $\mathbf{I_{1a}}$ may also undergo olefin and product coordination to provide the inactive reservoirs **2b** and **3b**. This proposed partitioning of the substrate-bound intermediate $\mathbf{I_1}$ into two entities is supported not only by the computational results but also helps to rationalize deuterium isotope effects observed previously for the mono-*N*-protected amino acid ligand systems.[2c] While the reaction in the presence of ligand gave positive isotope effects, the absolute magnitude of the effect varied from one the ligand system to another and was not in keeping with the strong normal isotope effect predicted if the C−H abstraction step is categorically rate-determining. This effect will be modulated if both the ligand-dependent N−H activation and the subsequent C−H activation steps contribute to the rate. It has been demonstrated that observations of isotope effects via global kinetics of complex multistep reaction networks may be difficult to attribute to a single step unless multiple isotope effect measurements may be made.[10] The overall kinetic rate law we determined holds for the case where $\mathbf{I_1}$ exists as two species $\mathbf{I_{1a}}$ and $\mathbf{I_{1b}}$. We propose that subtle differences in the intrinsic rates of ligand N−H and substrate C−H activation for the different ligand systems rationalize the kinetic, computational, and spectroscopic results. Incorporating these features into Scheme 2 results in the revised catalytic cycle of Scheme 4.

dx.doi.org/10.1021/ja207634t | *J. Am. Chem. Soc.* 2012, 134, 4600−4606

Scheme 4. Proposed Reaction Mechanism Highlighting Dual Rate-Determining Steps and Off-Cycle Catalyst Reservoirs

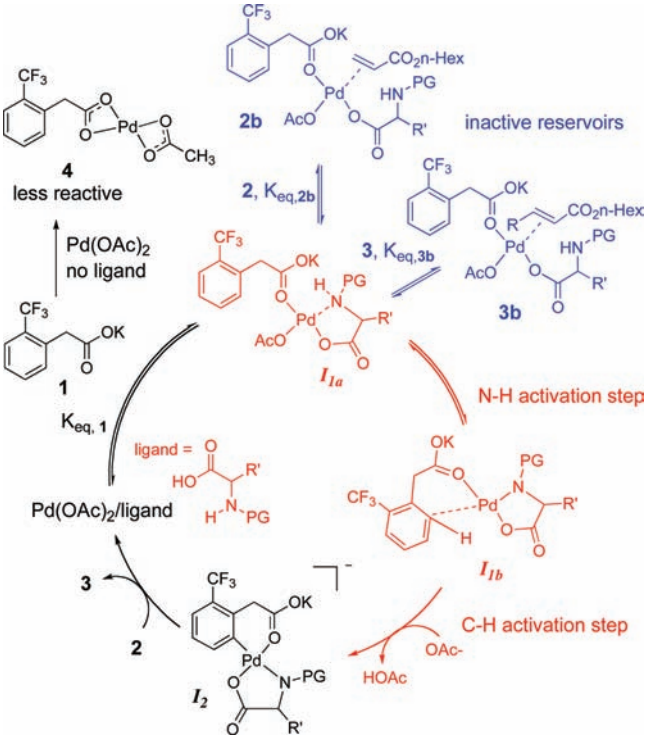

CONCLUSIONS

In summary, detailed kinetic studies based on reaction progress concentration profiles coupled with NMR spectroscopic studies provide an expanded mechanistic picture of the C−H activation reaction of Scheme 1. Suppressing formation of a stable mixed acetate species by introduction of mono-*N*-protected amino acid ligands accounts for the observed rate acceleration. Novel graphical manipulations of the data allow information about reaction orders to be extracted from concentration profiles without the requirement to convert the data to reaction rate. The empirical power-law form of the rate expression aids in proposing a series of elementary steps. Consideration of the steady-state rate expression in conjunction with reaction progress data allows rationalization of the unusual rate observations,[12] as well as clarifying observed differences in kinetic isotope effects for different ligand systems. Zero order dependence on [**1**] and [O_2], first order dependence on [Pd], and negative dependences on [**2**] and [**3**] are attributed to the presence of off-cycle reservoirs containing the substrate and product olefin species bound to a Pd carboxylate formed from interaction of **1** with the catalyst. While these off-cycle species suppress reaction rate, they may also play a role in maintaining catalyst stability by suppressing irreversible catalyst deactivation. The proposal that the rate-determining step involves an interplay between N−H and C−H activation processes helps to explain both the similar form of the rate expression, as well as the observed differences in absolute magnitude of rate, for the different amino acid ligands.

ASSOCIATED CONTENT

Supporting Information

Details of the experimental procedures and kinetic analysis. This material is available free of charge via the Internet at http://pubs.acs.org.

AUTHOR INFORMATION

Corresponding Author

blackmond@scripps.edu

Notes

The authors declare no competing financial interest.

ACKNOWLEDGMENTS

J.-Q.Y. gratefully acknowledges support from National Science Foundation under the Center of Chemical Innovation in Stereoselective C−H Functionalization (CHE-0943980). We acknowledge D.-H. Huang and L. Pasternack (TSRI NMR Facility) for valuable assistance with NMR spectroscopy and Dr. J. Bures for help with NMR data analysis.

REFERENCES

(1) For selected reviews of Pd-catalyzed C−H functionalization, see: (a) Campeau, L.-C.; Stuart, D. R.; Fagnou, K. *Aldrichimica Acta* **2007**, *40*, 35. (b) Satoh, T.; Miura, M. *Chem. Lett.* **2007**, *3*, 200. (c) Seregin, I. V.; Gevorgyan, V. *Chem. Soc. Rev.* **2007**, *36*, 1173. (d) Chen, X.; Engle, K. M.; Wang, D.-H.; Yu, J.-Q. *Angew. Chem., Int. Ed.* **2009**, *48*, 5094. (e) Ackermann, L.; Vicente, R.; Kapdi, A. R. *Angew. Chem., Int. Ed.* **2009**, *48*, 9792. (f) Daugulis, O.; Do, H.-Q.; Shabashov, D. *Acc. Chem. Res.* **2009**, *42*, 1074. (g) Lyons, T. W.; Sanford, M. S. *Chem. Rev.* **2010**, *110*, 1147. (h) Jia, C.; Kitamura, T.; Fujiwara, Y. *Acc. Chem. Res.* **2001**, *34*, 633.

(2) (a) Wang, D.-H.; Engle, K. M.; Shi, B.-F.; Yu, J.-Q. *Science* **2010**, *327*, 315. (b) Engle, K. M.; Wang, D.-H.; Yu, J.-Q. *Angew. Chem., Int. Ed.* **2010**, *49*, 6169. (c) Engle, K. M.; Wang, D.-H.; Yu, J.-Q. *J. Am. Chem. Soc.* **2010**, *132*, 14137.

(3) (a) Lu, Y.; Wang, D.-H.; Engle, K. M.; Yu, J.-Q. *J. Am. Chem. Soc.* **2010**, *132*, 5916. (b) Lu, Y.; Leow, D.; Wang, X.; Engle, K. M.; Yu, J.-Q. *Chem. Sci.* **2011**, *2*, 967. (c) Dai, H.-X.; Stepan, A. F.; Plummer, M. S.; Zhang, Y.-H.; Yu, J.-Q. *J. Am. Chem. Soc.* **2011**, *133*, 7222. (d) Huang, C.; Chattopadhyay, B.; Gevorgyan, V. *J. Am. Chem. Soc.* **2011**, *133*, 12406. (e) Engle, K. M.; Thuy-Boun, P. S.; Dang, M.; Yu, J.-Q. *J. Am. Chem. Soc.* **2011**, *133*, 18183. (f) Novák, P.; Correa, A.; Gallardo-Donaire, J.; Martin, R. *Angew. Chem., Int. Ed.* **2011**, *50*, 12236.

(4) (a) Ferreira, E. M.; Stoltz, B. M. *J. Am. Chem. Soc.* **2003**, *125*, 9578. (b) Stuart, D. R.; Fagnou, K. *Science* **2007**, *316*, 1172. (c) Zhang, Y.-H.; Shi, B.-F.; Yu, J.-Q. *J. Am. Chem. Soc.* **2009**, *131*, 5072. (d) Izawa, Y.; Stahl, S. S. *Adv. Synth. Catal.* **2010**, *352*, 3223.

(5) (a) Hickman, A. J.; Sanford, M. S. *ACS Catal.* **2011**, *1*, 170. (b) Jintoku, T.; Taniguchi, H.; Fujiwara, Y. *Chem. Lett.* **1987**, *16*, 1159. (c) Eberson, L.; Jonsson, E. *Acta Chem. Scand. Ser. B* **1974**, *28*, 771. (d) Ye, M.; Gao, G.-L.; Yu, J.-Q. *J. Am. Chem. Soc.* **2011**, *133*, 6964.

(6) Musaev, D. G.; Kaledin, A.; Shi, B.-F.; Yu, J.-Q. *J. Am. Chem. Soc.* **2012**, *134*, 1690.

(7) See Supporting Information for details.

(8) (a) Blackmond, D. G. *Angew. Chem., Int. Ed.* **2005**, *44*, 4302. (b) Mathew, J. S.; Klussmann, M.; Iwamura, H.; Valera, F.; Futran, A.; Emanuelsson, E. A. C.; Blackmond, D. G. *J. Org. Chem.* **2006**, *71*, 4711.

(9) Zotova, N.; Broadbelt, L. J.; Armstrong, A.; Blackmond, D. G. *Bioorg. Med. Chem. Lett.* **2009**, *19*, 3934.

(10) Jones, W. D. *Acc. Chem. Res.* **2003**, *36*, 140.

(11) Rosner, T.; Le Bars, J.; Pfaltz, A.; Blackmond, D. G. *J. Am. Chem. Soc.* **2001**, *123*, 1848.

(12) Unusual concentration dependences were also observed in Pd(II)-mediated C−H functionalization: Deprez, N. R.; Sanford, M. S. *J. Am. Chem. Soc.* **2009**, *131*, 11234.